

1
2
3
4
5
6
7
8
9
10
11
12
13
14
15
16
17
18
19
20
21
22

Supporting Information

Linking Increased Isotope Fractionation at Low

Concentrations to Enzyme Activity Regulation:

4-Cl Phenol Degradation by *Arthrobacter*

chlorophenolicus A6

Kankana Kundu, Aileen Melsbach, Benjamin Heckel, Sarah Schneidermann, Dheeraj Kanapathi,

Sviatlana Marozava, Juliane Merl-Pham, Martin Elsner

SUMMARY

12 pages, 7 figures

CONTENT

Materials and Methods

HPLC method for 4-CP concentration measurement

Estimation of growth kinetic parameters

EA-IRMS measurement for determination of reference values

Method for analysis of the carbon isotope in 4-CP samples

Lipid extraction and membrane fatty acid analysis

Proteomics analysis

Supporting Figures

Figure S1. Schematic diagram of custom-made bioreactor used in this study.

23 Figure S2. Degradation of four chlorophenol and cell concentration in batch cultivation
24 experiment. The circle denotes the sampling point for fatty acid and proteome analysis
25 Figure S3: The observed specific growth rate at different residual 4-CP concentrations in
26 batch was modelled using Haldane inhibition¹ kinetics.
27 Figure S4. Degradation profile of 4-chlorophenol at 95 $\mu\text{g L}^{-1}$ shows slow enzymatic
28 turn-over.
29 Figure S5. Change in morphology at different dilution points in chemostats and batch
30 Figure S6. Non-parametric clustering (NMDS) of all conditions used for proteomics
31 analysis.
32 Figure S7: Heat map representing the clustering of quantified proteins (in total 1201) in
33 all samples
34 Figure S8: Voom transformation of the proteomics data.
35 Figure S9: GC-IRMS chromatogram of low concentration-extracts
36
37 Supporting Tables
38 S1Table S1-S5 – Tables for proteomics data analysis. Provided as an excel file.
39 SI Table S6 – Biomass and yield measured at different dilution rates after achieving steady states
40 in chemostat.
41
42 Supporting References

43

44 **SI Materials and methods:**

45 **HPLC method for 4-CP concentration measurement**

46 The eluents were acetonitrile, as well as water acidified with 1% of acetic acid. The initial gradient
47 contained 10% acetonitrile (1 min) and was increased to 80% acetonitrile (2-6 min), after which
48 the level was maintained for 3 min. The gradient was returned to 10% acetonitrile (8-13 min) with
49 a post-time run (13-16 min). The injected sample volume was 20 μL . The flow rate was 0.7 mL
50 min^{-1} , and oven temperature was set to 45 °C. The compounds were detected by UV absorbance
51 at 222 nm, and the peaks quantified using LabSolutions V 5.71 SP2 (Shimadzu Corp., Japan).

52 **Estimation of growth kinetic parameters**

53 Growth kinetics of *A. chlorophenolicus* A6 was described by Haldane kinetics¹

54
$$\mu = \frac{\mu_{max} \cdot S}{(S + K_S) \cdot (1 + \frac{S}{K_I})} \quad (1)$$

55 where μ is the specific growth rate, S is the substrate (i.e., 4-CP) concentration, μ_{max} is the
56 maximum growth rate, K_S is the substrate affinity and K_I is an inhibition constant. The three
57 parameter K_S , K_I and μ_{max} were estimated from fitting the experimentally measured μ and S (i.e.,
58 4-CP concentration) in batch experiments to the model (eq.1). The specific growth rate was
59 calculated as

60
$$\mu = \frac{dC_x/dt}{C_x} \quad (2)$$

61 where C_x is the cell concentration. The model implementation, fitting parameter estimations and
62 model analysis was performed using Python and employing the built-in functions in scientific
63 libraries NumPy and SciPy². The three parameters parameter K_s , K_I and μ_{max} in the Haldane
64 kinetics model (eq.1) were estimated from the experimentally measured μ and S (4-CP
65 concentration) data by minimizing the Root mean squared error (RMSE) as objective function.

$$66 \quad \text{RMSE} = \sqrt{\frac{\sum(\vartheta_{exp} - \vartheta_{sim})^2}{N}} \quad (3)$$

67 The “brute force” optimization method was used to find the global minimum of the objective
68 function to compute the objective function’s value at each point of a multidimensional grid of
69 points, to obtain the global minimum of the function. This multidimensional grid contained
70 ranges of μ_{max} (0.002 to 0.9), K_i (1 to 100) and K_s (0.5 to 100) with linear grid space of 0.005
71 and 1, respectively. Thereafter, the result of “brute force” minimization was fed as initial guess
72 to obtain a more precise (local) minimum using the downhill simplex algorithm³.

73 **EA-IRMS measurement for determination of reference values**

74 4-CP (Sigma-Aldrich, Germany) used in the cultivation was characterized with elemental analyzer
75 coupled with isotope ratio mass spectrometry (EA-IRMS), which was used as a standard for
76 isotope analysis during ongoing degradation. A EuroEA (Euro Vector, Milano, Italy) was coupled
77 with Finnigan MAT 253 IRMS via a FinniganTM ConFlow III interface (Thermo Fisher Scientific,
78 Bremen, Germany). Calibration of standards was performed against the organic referencing
79 materials USG 40 (L-glutamic acid), USG 41 (L-glutamic acid) and IAEA 600 (caffeine) provided
80 by the International Atomic Energy Agency (IAEA, Vienna). $\delta^{13}\text{C}$ of 4-CP in per mil (‰) relative
81 to PeeDee Belemnite (V-PDB) by using the following equation-

82

$$\delta^{13}\text{C} = \frac{\left(\frac{\text{c}^{13}}{\text{c}^{12}}\right)_x}{\left(\frac{\text{c}^{13}}{\text{c}^{12}}\right)_{\text{ref}}} - 1 \quad (2)$$

83 Determination of $\delta^{13}\text{C}$ values was relative to the laboratory CO_2 monitoring gas, which was
84 introduced at the beginning and the end of each analysis run. The laboratory CO_2 was calibrated
85 to VPDB by reference CO_2 standard (RM8563) supplied by the IAEA. 4-CP samples were
86 measured four times, and the instrumental isotope values of 4-CP $\delta^{13}\text{C} = -28.12\text{‰} \pm 0.03\text{‰}$.

87 **Method for analysis of the carbon isotope in 4-CP samples**

88 The IRMS was set to a vacuum of 1.9×10^{-6} mbar, an accelerating potential of 9 kV and an
89 emission energy of 2 mA. Helium grade 5.0 was used as a carrier gas with a flow rate of 1 mL
90 min^{-1} . Liquid samples (volume in between 1 to 2 μL) were injected with a GC pal autosampler
91 (CTC analytics). The injector was held at 200°C with a split ratio of 1:10. The GC program was
92 as follows: start 70°C (hold 1 min), ramp 1 $15^\circ\text{C}/\text{min}$ to 130°C (hold for 1 min), ramp 2 $40^\circ\text{C}/\text{min}$
93 to 220°C (hold for 3.5 min). GC-program: start 80°C (hold 4 min) \rightarrow ramp 1 $4^\circ\text{C}/\text{min}$ to 150°C
94 (hold for 5 min) \rightarrow ramp 2 $2^\circ\text{C}/\text{min}$ to 200°C (hold for 1 min). A commercial ceramic tube/reactor
95 with CuO/NiO/Pt-wire (Thermo Fisher Scientific, Bremen, Germany) operated at 940°C was used
96 for isotope analysis. Prior to the isotope analysis, the reactor was oxidized at 940°C for 6 hours.
97 Determination of $\delta^{13}\text{C}$ values for all the samples was relative to our laboratory CO_2 monitoring
98 gas, as described earlier (eq.2).

99 **Lipid extraction and membrane fatty acid analysis**

100 A sample volume of 2 ml was centrifuged at 4°C for 10 min. The fatty acids were separated from
101 the rest of the lipid by saponification with sodium hydroxide. To this end, the bacterial pellet was

102 treated with 1 mL of a solution consisting of 45 g of NaOH in 150 mL of methanol and 150 mL of
103 MilliQ water. The mixture was vortexed briefly, heated in a water bath (100 °C, 5 min), vigorously
104 vortexed for 5-10 seconds and heated again for another 25 min in the water bath (100 °C). To
105 methylate the saponified free membrane fatty acids and generate FAMES, 2 mL of a solution
106 consisting of 6.0 N HCl and methanol in a volumetric ratio of 1.2:0.8 was added and after brief
107 vortexing, the sample was heated at 80 °C (10 min) in the water bath again. After rapidly cooling
108 the sample in running water, the generated FAMES were extracted from the bacterial cell
109 membrane by adding 1.25 mL of a mixture of hexane and diethyl ether (1:1, v/v) and gentle
110 tumbling in a rotator (10 min). The aqueous lower phase (containing other cell components) was
111 discarded. Subsequently, the organic phase was base-washed with at least 3.0 mL of a solution of
112 10.8 g NaOH in 900 mL H₂O. The sample was mixed again in a rotator for 5 min. Two third of
113 the upper, organic phase containing FAME was transferred into a 1 mL GC Vial containing a
114 200 µL inlay and was analyzed using a GC-MS equipped with a split/ splitless injector
115 (FinniganTrace Ultra and Trace DSQ, Thermo Electron Cooperation, Waltham, MA, USA). To
116 separate the FAMES, a CP-Sil 88 capillary column was used (from Agilent Technologies,
117 Netherlands; length, 50 m; inner diameter, 0,25 mm; 0,20 µm film). The GC conditions were as
118 follows: the detector temperature was held at 200 °C, and the injector temperature was held at
119 240 °C. The injection was splitless for 1 min, and the carrier gas was helium at a flow of 0.3 mL
120 min⁻¹. The temperature program was as follows: 40 °C, 3 min isothermal; 6 °C min⁻¹ to 220 °C and
121 finally 4 min at 220 °C isothermal. The pressure program was as follows: 186 kPa, 2 min isobaric;
122 4 kPa min⁻¹ to 310 kPa and finally 3 min at 310 kPa isobaric. To determine the relative amounts
123 of FAMES, the peak areas of the fatty acids in total were used.

124 **Proteomics analysis**

125

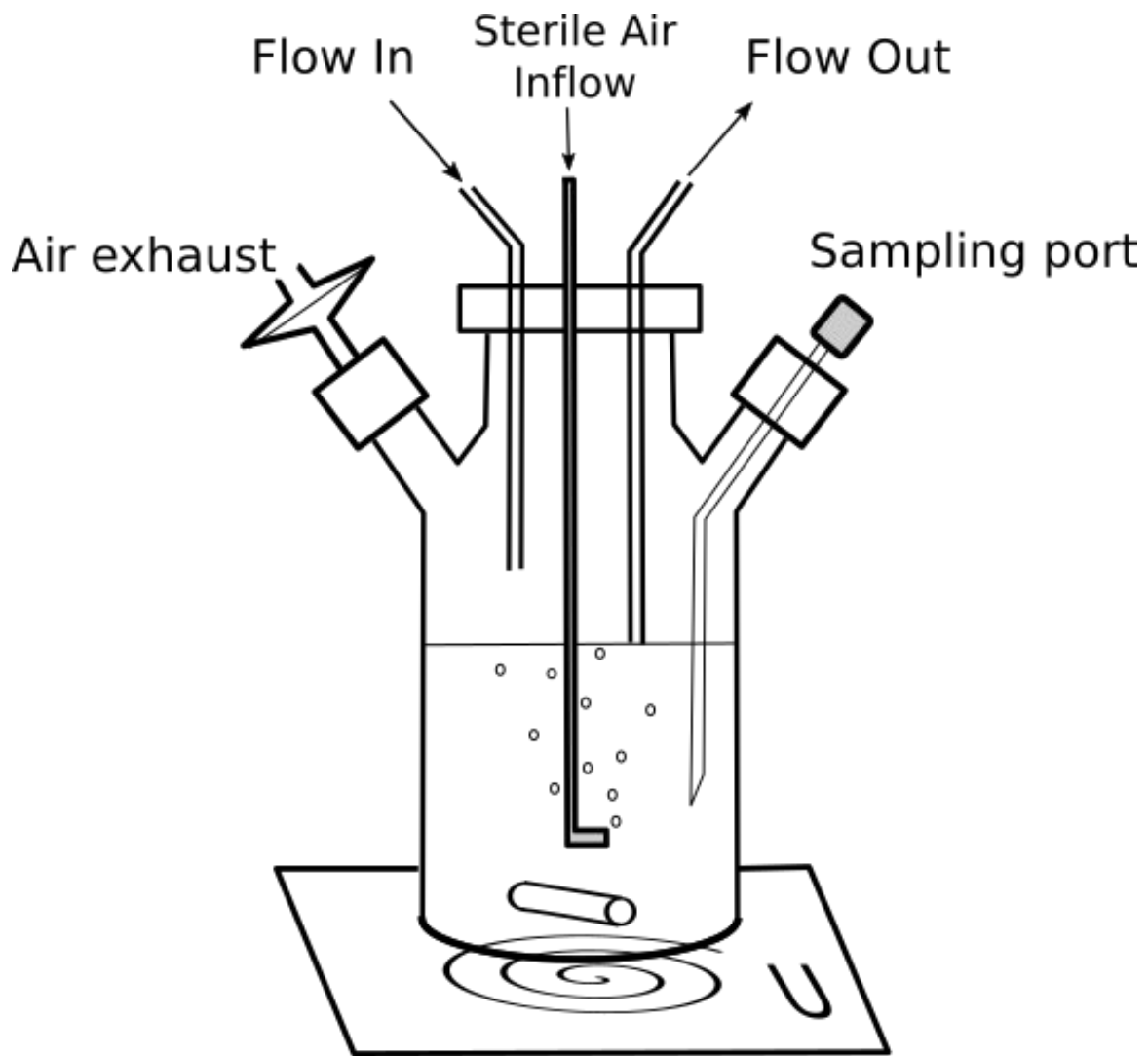
126 LC-MS/MS analysis was performed on a QExactive HF mass spectrometer (Thermo Fisher
127 Scientific) online coupled to an Ultimate 3000 nano-RSLC (Thermo Scientific). The acquired
128 spectra were loaded to the Progenesis QI software (version 4.0, Nonlinear Dynamics, part of
129 Waters) for label-free quantification and analyzed as described previously ⁴. All MS/MS spectra
130 were exported as Mascot generic files and used for peptide identification with Mascot (version
131 2.6.2) in the UniProt *A. chlorophenolicus* A6 protein database (1479563 residues, 4608
132 sequences). Search parameters used were: 10 ppm peptide mass tolerance and 0.02 Da fragment
133 mass tolerance, one missed cleavage allowed, carbamidomethylation was set as fixed
134 modification, methionine oxidation and asparagine or glutamine deamidation were allowed as
135 variable modifications. A Mascot-integrated decoy database search calculated an average false
136 discovery of 0.59 % when searches were performed with the mascot percolator algorithm and
137 $p < 0.05$. Peptide assignments were re-imported into the Progenesis QI software. Raw abundance
138 data of all unique peptides allocated to each protein were normalized and summed up.

139

140

141

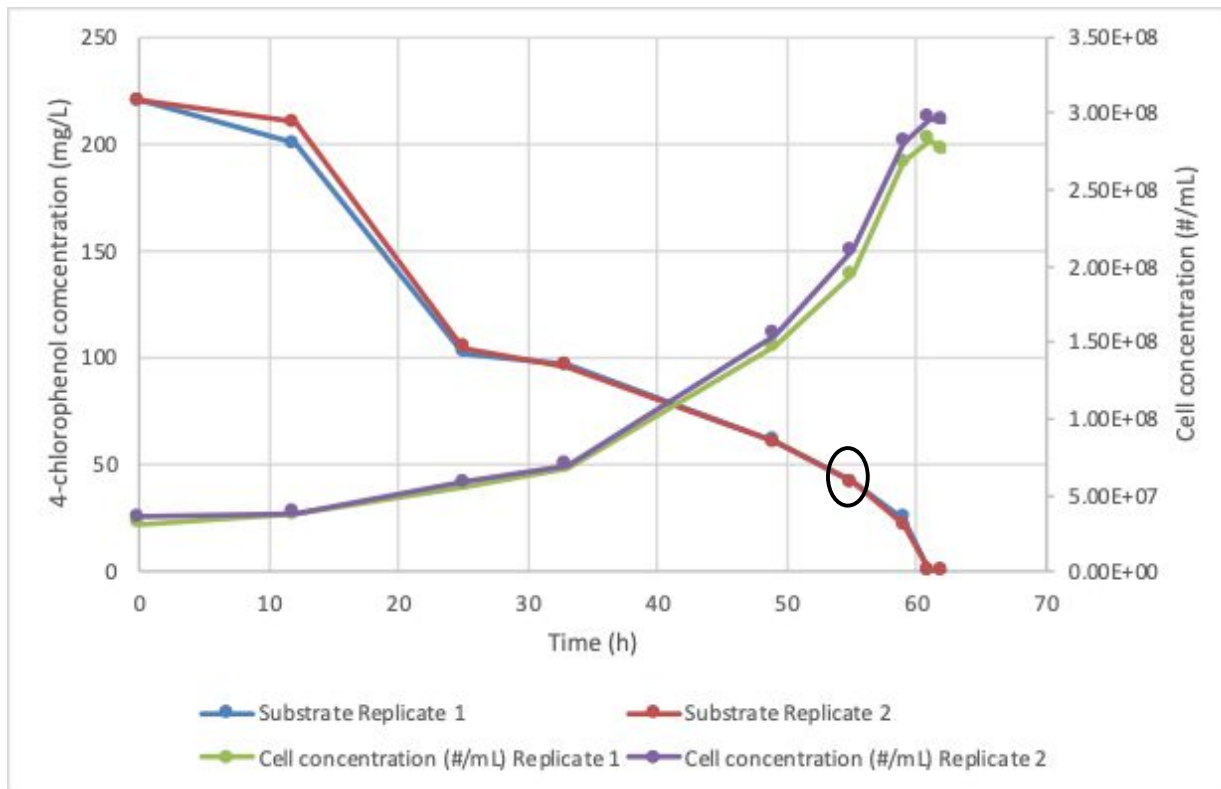
142 **SI Figures:**



143

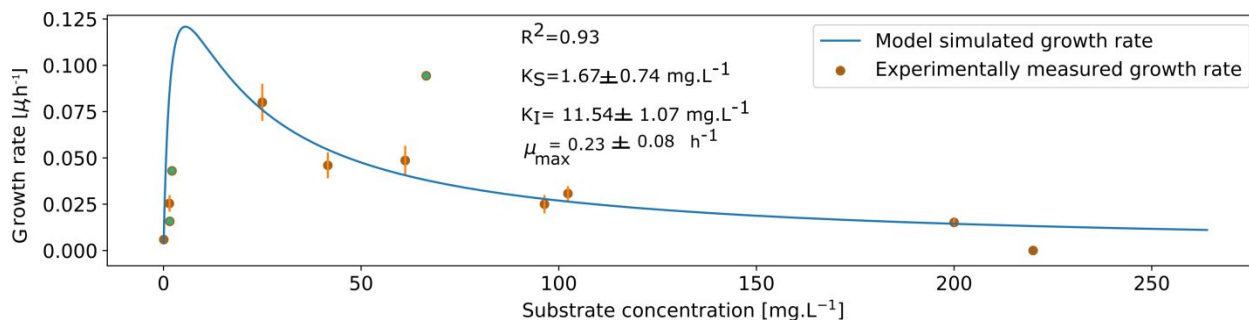
144 **Figure S1:** Schematic diagram of custom-made bioreactor used in this study.

145



146

147 **Figure S2:** Degradation of 4 chlorophenol and cell concentration in batch cultivation experiment.
 148 After a lag phase of 12 hours, a slow increase in cell concentrations was observed at $\sim 100 \text{ mg L}^{-1}$
 149 4-CP (transition lag phase), whereas growth became rapid (exponential phase) at lower 4-CP
 150 concentrations of $\sim 40 \text{ mg L}^{-1}$. The circle denotes the sampling point for fatty acid and proteome
 151 analysis.

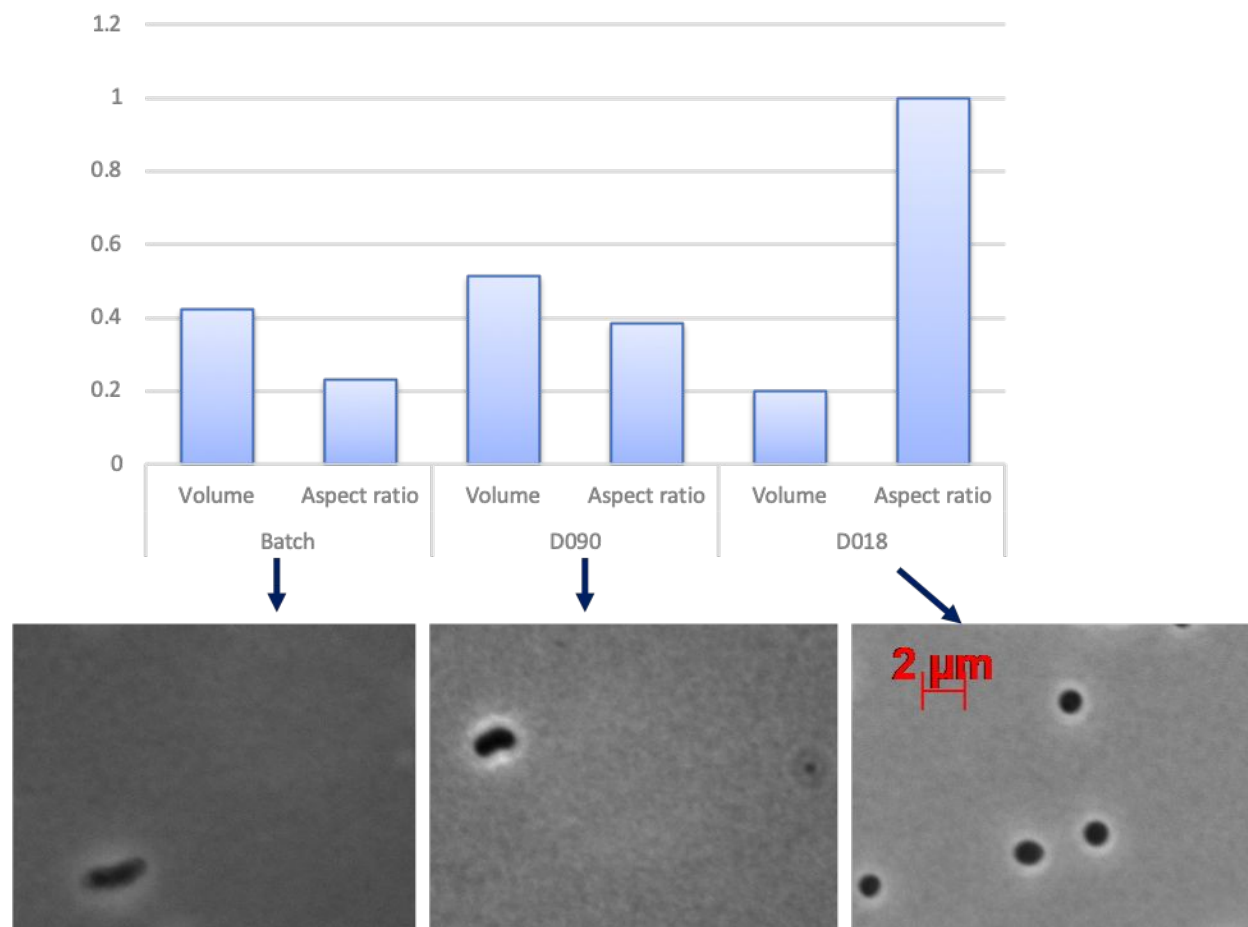


152

153 **Figure S3:** The observed specific growth rate at different residual 4-CP concentrations in batch
 154 was modelled using Haldane inhibition¹ kinetics. The symbols indicate observed growth rate (μ ,
 155 calculated according to eq.2) based on cell concentrations and residual substrate (4-chlorophenol)
 156 concentration in batch cultivation. The line indicates μ according to Haldane inhibition kinetics
 157 model (eq. 1) using fitted growth parameters of (μ_{\max}), Monod affinity constant (K_s) and

158 inhibition constant (K_I) in batch cultivation. Data points represent the mean \pm standard deviation
159 of samples. The fitted kinetic parameters imply that 4-CP concentrations above $K_I \sim 12.0 \text{ mg L}^{-1}$
160 (0.09 mM) reduce growth of *A. chlorophenolicus* A6. Symbols in green indicate growth rates
161 observed in chemostat cultivations (Fig.1, see the main manuscript).

162



163

164

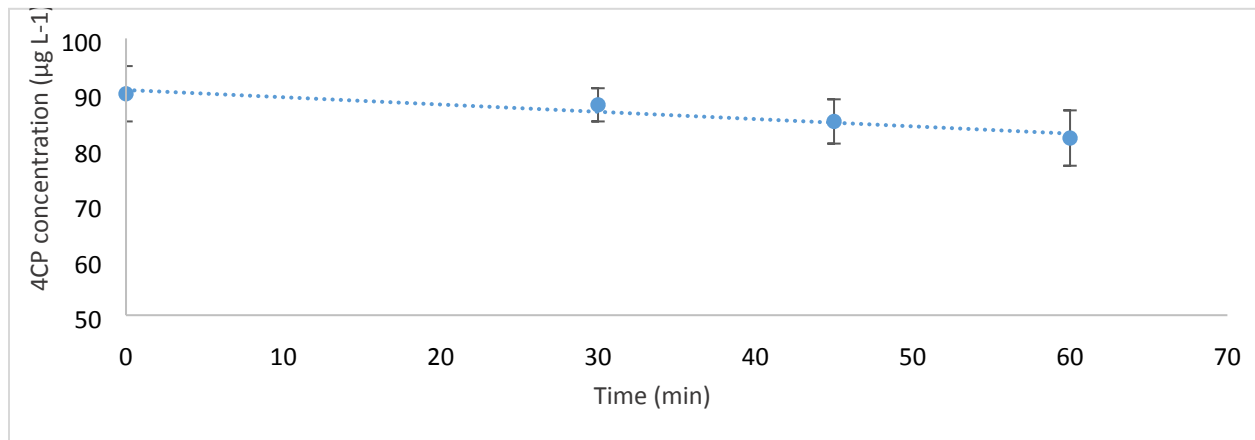
165 **Figure S4:** .Change in morphology at different dilution points in chemostats and batch. D090 and
166 D018 denote dilution rate of 0.090 and 0.018 h^{-1} , respectively.

167

168

169

170



171

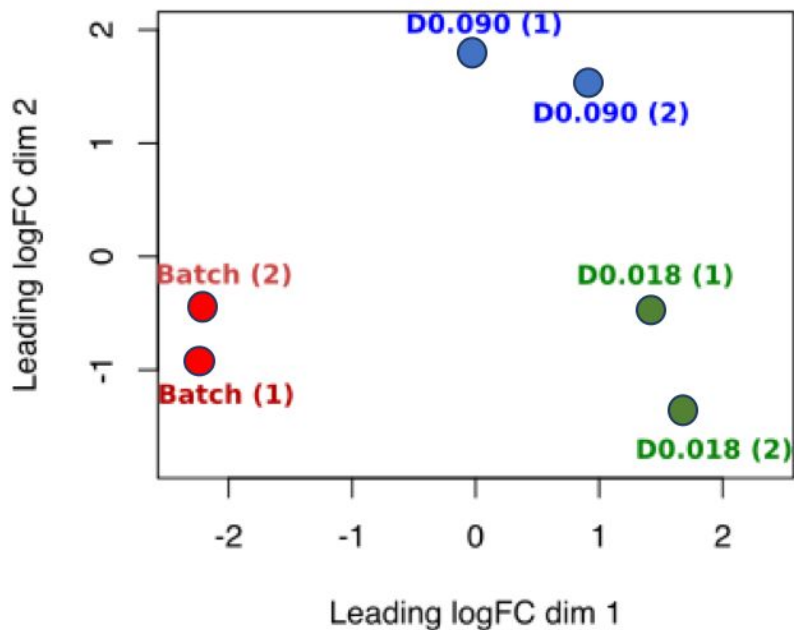
172 **Figure S5:** Degradation profile of 4-chlorophenol with an effluent concentration of 95 µg L⁻¹
173 in the chemostat under no addition of feed shows slow enzymatic turn-over.

174

175

176

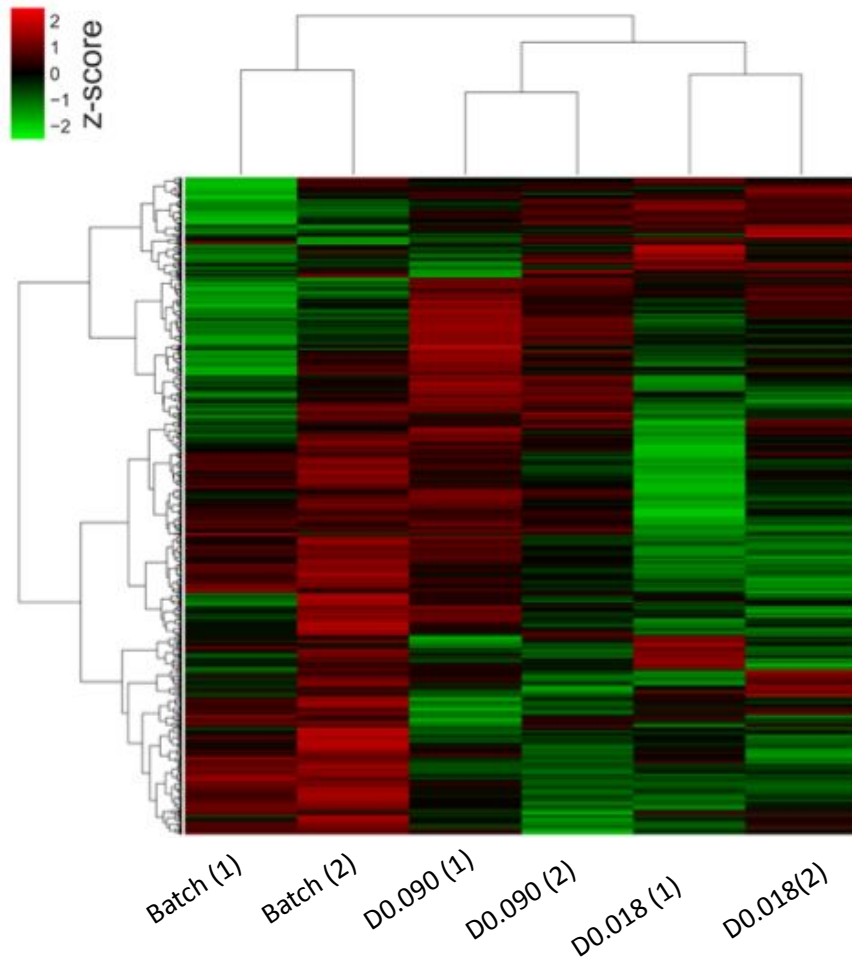
177



178

179 **Figure S6:** Non-parametric clustering (NMDS) of all conditions used for proteomics analysis. The
180 biological replicates are placed closer on the plot, which shows similarity, hence, can be used for
181 further analysis. The similar clustering between biological replicates are shown in Fig.S6 based on

182 Euclidean distance. The correlation coefficient was similarly high in biological replicates (0.9 for
183 Batch, D0.018 and 0.7 for D0.090)



184

185

186 Fig. S7: Heat map representing the clustering of quantified proteins (in total 1201) in all samples

187 - Batch, D0.018 and D0.09. Protein abundance is displayed in the heat map as z-scores (i.e.,

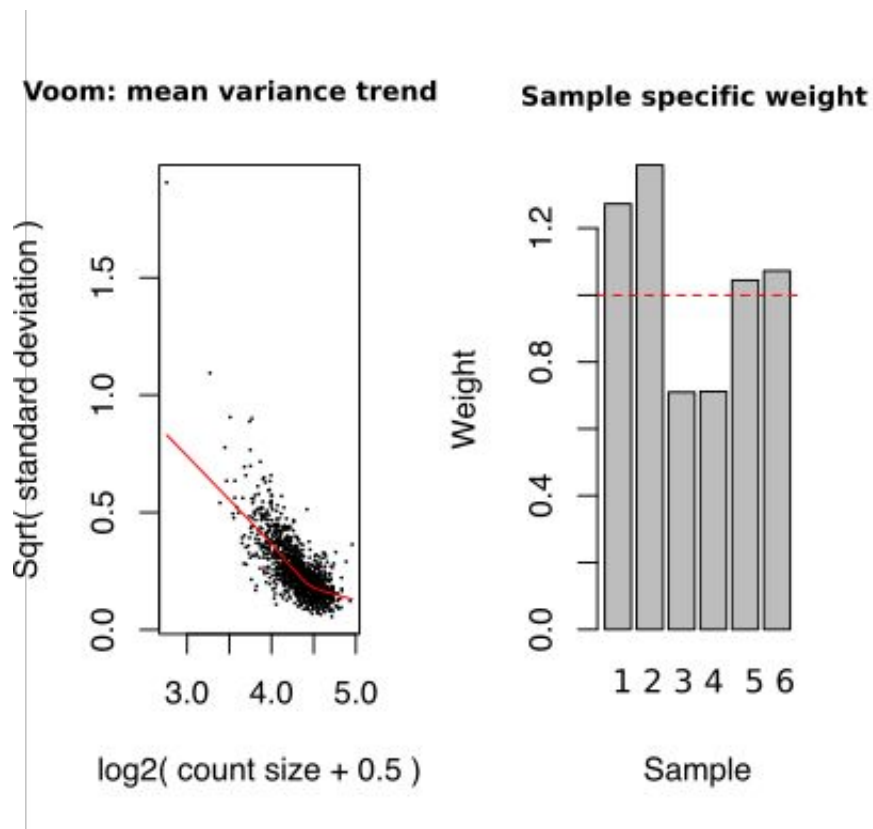
188 calculated based on how many SD units a protein's abundance is away from the mean abundance

189 derived from all conditions) in the range between 2 (of significantly higher abundance, red) and -

190 2 (of significantly lower abundance, green). Each batch and chemostat cultivation was performed

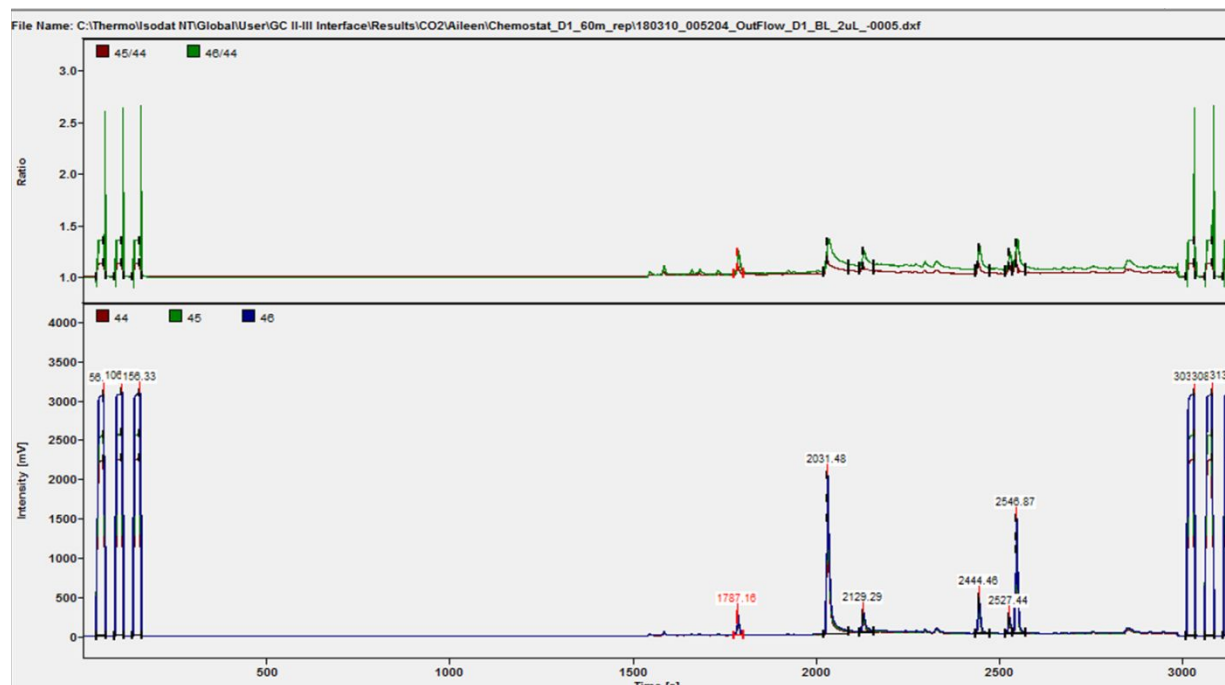
191 in replicates as indicated by dilution rates in the brackets below the heat map.

192



194

195 **Figure S8:** Voom transformation of the proteomics data. Mean variance trend in the data is shown
 196 (left panel) and down weight low-intensity observation by implying sample-specific weight (right
 197 panel). 1,2: Batch replicates, 3,4 : two replicates for chemostat at D 0.018 h⁻¹ and 5,6: two
 198 replicates for chemostat at D0.090 h⁻¹.



199
 200 **Figure S9:** IRMS chromatograms from measurements of 4-Cl phenol extracts of 90 µg/L from
 201 chemostat samples. The 4-Cl peak appears at a retention time of 2031 seconds.

202

203 **SI Tables**

204 **Table S6** – Biomass and yield measured at different dilution rates after achieving steady states in
 205 chemostat.

| Dilution rate (h ⁻¹) | Biomass (mg L ⁻¹) | Yield (mg-Biomass ⁻¹ mg-substrate) |
|----------------------------------|-------------------------------|---|
| 0.018 | 6.012 | 0.0273 |
| 0.038 | 5.377 | 0.0245 |
| 0.090 | 1.933 | 0.0146 |

206

207 **REFERENCES**

208 (1) Haldane, J. B. S. *Enzymes*. 1930. *Repr. by MIT, Cambridge* **1965**.

209 (2) Oliphant, T. E. Python for Scientific Computing. *Comput. Sci. Eng.* **2007**, 9 (3), 10–20.
 210 <https://doi.org/10.1109/MCSE.2007.58>.

211 (3) Nelder, J. A.; Mead, R. A Simplex Method for Function Minimization. *Comput. J.* **1965**, 7
 212 (4), 308–313. <https://doi.org/10.1093/comjnl/7.4.308>.

213 (4) Merl, J.; Ueffing, M.; Hauck, S. M.; von Toerne, C. Direct Comparison of MS-Based
 214 Label-Free and SILAC Quantitative Proteome Profiling Strategies in Primary Retinal
 215 Müller Cells. *Proteomics* **2012**, 12 (12), 1902–1911.